5820 *Macromolecules* **2010**, *43*, 5820–5832
DOI: 10.1021/ma1005233

Macromolecules
ARTICLE

A Novel Stochastic Approach for the Prediction of the Exact Topological Characteristics and Rheological Properties of Highly-Branched Polymer Chains

Dimitrios Meimaroglou and Costas Kiparissides*

Department of Chemical Engineering, Aristotle University of Thessaloniki and Chemical Process Engineering Research Institute, P.O. Box 472, Thessaloniki, Greece 54124

Received October 16, 2009; Revised Manuscript Received May 26, 2010

ABSTRACT: A novel stochastic algorithm is described for the accurate prediction of the detailed molecular topology of highly branched polymer chains. Stochastic topological polymer chain simulations are carried out in conjunction with a polymerization kinetic MC simulator. Contrary to previous efforts on the stochastic simulation of topological features of branched polymer chains, the present approach does not apply any simplifying assumptions regarding the distributional form of "live" and "dead" polymer chain populations. The proposed stochastic approach takes explicitly into account the effects of various diffusional limitations in the termination and propagation rate constants (i.e., gel- and glass-effect) as well as the effect of branching density on the kinetics of various reactions (i.e., transfer to polymer and chain scission reactions). To demonstrate the predictive capabilities of the proposed stochastic approach, the free-radical polymerization of ethylene in an industrial high-pressure tubular reactor is investigated. It is shown that the present stochastic kinetic/topology algorithm can provide detailed information on the topological features of highly branched polymer chains (i.e, long- and short-chain branching distributions, segment seniority and priority distributions, etc.). The topological information, obtained by the application of the stochastic kinetic/topology algorithm, is then used together with a 3-D molecular random-walk simulator to predict the 3-D random spatial configurations of branched polymer chains as well as some important rheological parameters (i.e., the mean radius of gyration, R_g, the mean hydrodynamic radius, R_h, and the average branching factor, g) of low-density polyethylene.

Introduction

Control of the molecular architecture of polymer chains produced in a polymerization reactor is a subject of profound interest to polymer scientists and industry as well. This originates from the well-established fact that the molecular properties (e.g., molecular weight distribution (MWD), copolymer composition distribution (CCD), long-chain branching distribution (LCBD), etc.) are directly linked with the polymer end-use properties (e.g., physical, chemical, mechanical, rheological, etc.). Hence, the elucidation of the molecular architecture of highly branched polymer chains in terms of the kinetic mechanism and polymerization conditions (e.g., temperature, pressure, mixing, etc.) has been the subject of a great number of theoretical and experimental studies.

A well-known approach for the calculation of the distributed polymer molecular properties (e.g., MWD, LCBD, etc.) is the use of multivariate population balance equations (PBE).[1] In principle, dynamic PBEs can be derived to describe the time evolution of the "live" and "dead" polymer chains in a polymerization reactor in terms of a specific polymerization kinetic mechanism. In the open literature, a number of numerical methods have been proposed to reduce the resulting infinite system of differential equations into a low-order system. These include the kinetic lumping method,[2−4] the polynomial expansion method,[5] the global orthogonal collocation,[6] the method of moments,[7,8] the "numerical fractionation" method,[9,10] the discrete weighted Galerkin[11,12] and the orthogonal collocation on finite elements and sectional grid methods.[13] Despite their computational complexities, in a series of recent publications,[14−16] the application of orthogonal collocation on finite elements and fixed pivot methods to free-radical linear and nonlinear polymerization systems was demonstrated.

An alternative approach to the above deterministic methods is the use of probabilistic tools (e.g., Monte Carlo simulations). Stochastic simulations have attracted significant attention over the last 30 years, due to their inherent capability to simulate the discrete and random nature of polymerization kinetics. The application of MC methods to complex polymerization systems has been facilitated by the dramatic increase in computer power that has gradually eliminated the main disadvantage of stochastic methods associated with their high computational requirements. It should be pointed out that stochastic simulations have an additional advantage over the commonly employed deterministic numerical methods for they can deal with multidimensional problems (e.g., three- and/or higher-dimensional problems) in a simple and efficient way, making them ideal computational tools for the calculation of the multidimensional distributed molecular properties (i.e., joint MW−LCB distribution, joint MW−CC distribution, etc.). In the past, a number of different stochastic approaches have been proposed[17,18] and applied to both homopolymerization[19−21] and copolymerization[22−25] systems. However, in most cases, a number of simplifying kinetic and chain distributional assumptions have been applied to facilitate the stochastic numerical solution.

In principle, the average and distributed molecular properties of polymer chains in a polymerization system (e.g., M_n, M_w, MWD, CCD, etc.) can be calculated by using either deterministic or stochastic numerical methods. However, a number of molecular properties (i.e., the topology and distribution of short- and long-chain branches, the branching order distribution, etc.) that

*Corresponding author. Tel: + 302310 99 6211; fax: +2310 99 6198; e-mail: cypress@alexandros.cperi.certh.gr.

 Published on Web 06/15/2010 © 2010 American Chemical Society

are directly linked with the molecular architecture of polymer chains cannot be calculated and, often, cannot even be measured experimentally. However, such molecular topological properties, including the length and branching order distributions of short- and long-chain branches, attached to the main backbone of a highly branched polymer chain, can strongly affect, i.e., the rheological behavior and, thus, the polymer melt processability.

Recently, significant advances have been made on the rheological behavior of highly branched polymer melts.[26−31] However, the application of the proposed rheological models and theories is bounded by the assumed structure of the branched polymer chains, since there is limited theoretical or/and experimental information regarding the molecular topological characteristics of nonlinear polymer chains. Hence, the ability to accurately predict the topological characteristics of highly branched polymer chains, in terms of the kinetic mechanism and reactor operating conditions, is of profound theoretical and industrial importance since, in principle, the rheological behavior of polymer melts can be assessed in terms of the calculated topological properties of highly branched polymer chains.[28−31]

The first notable attempt to predict the molecular architecture of highly branched polymer chains was reported by Tobita[32,33] who employed a "random sampling technique" to generate long polymer chains via the successive connection of linear chain segments (also called "primary polymers"). Tobita's approach, although powerful in providing detailed molecular structural characteristics, was limited by the fact that the generation of "primary polymer" segments was assumed to take place under constant polymerization conditions, following a priori known distributional forms (i.e., of the most probable distribution). The former limitation was addressed by Inkson,[34] who developed a MC algorithm based on Tobita's approach, to simulate stochastically a time-varying catalytic olefin polymerization system. Moreover, Iedema and his co-workers[35,36] described a graph-based approach for efficient storage of relevant topological information regarding a polymer chain while the chain length and branching distributions of the macromolecular segments were calculated via the implementation of a Galerkin on finite elements method. Although Iedema's work provided a good approximation of the molecular properties of branched polymers, the number of assumptions, made to simplify the actual implementation of the method, limited its general applicability and predictive capabilities. These limitations were associated with the application of the method to nondynamic polymerization systems, the requirement for a priori knowledge of the analytical functions for segment length and branching order distributions, the assumption of random scission of the "primary polymer" chains and the inaccurate handling of termination by combination reactions. In a recent publication by the same group,[37] the random segment connection algorithm was replaced by a "backtracking algorithm" that displayed limited applicability to actual polymerization processes due to their complex kinetic mechanisms. From the above points, it becomes apparent that the accurate prediction of the exact topological characteristics of highly branched polymer chains, in a time-varying polymerization system, has been partially dealt, and thus, the problem remains unsolved in its general form.

In the present work, a combined kinetic/topology stochastic algorithm is developed for the accurate prediction of the complete topological architecture of highly branched polymer chains. The stochastic polymer chains topological simulator proceeds in complete conjunction with the polymerization kinetic mechanism, without making any assumptions on the distributional functions of "live" and "dead" polymer chains. Branched polymer chains are constructed via a detailed monomer-addition process, taking into account the various diffusional phenomena (i.e., gel-effect, glass-effect) associated with the respective termination and propagation rate constants. Note that the proposed algorithm is quite general and can be applied to any complex polymerization system (e.g., free-radical, catalytic, etc.) under time-varying polymerization conditions (e.g., temperature, pressure, species concentrations, etc.).

The Polymerization Kinetic Mechanism

To describe the formation of both linear and highly branched polymer chains, in a chemically initiated free-radical polymerization system, the following general kinetic mechanism was employed.

Initiator Decomposition.

$$\mathrm{I} \xrightarrow{k_d} 2\mathrm{PR}^{\bullet} \tag{1}$$

Chain Initiation.

$$\mathrm{PR}^{\bullet} + \mathrm{M} \xrightarrow{k_I} \mathrm{P}_{0,1} \tag{2}$$

Propagation.

$$\mathrm{P}_{b,n} + \mathrm{M} \xrightarrow{k_p} \mathrm{P}_{b,n+1} \tag{3}$$

Chain Transfer to Monomer.

$$\mathrm{P}_{b,n} + \mathrm{M} \xrightarrow{k_{fm}} \mathrm{D}_{b,n} + \mathrm{P}_{0,1} \tag{4}$$

Chain Transfer to Solvent (Chain Transfer Agent).

$$\mathrm{P}_{b,n} + \mathrm{S} \xrightarrow{k_{fs}} \mathrm{D}_{b,n} + \mathrm{P}_{0,1} \tag{5}$$

Reaction with Terminal Double-Bond.

$$\mathrm{P}_{b,n} + \mathrm{D}_{r,m} \xrightarrow{k_{db}} \mathrm{P}_{b+r+1,n+m} \tag{6}$$

Chain Transfer to Polymer.

$$\mathrm{P}_{b,n} + \mathrm{D}_{r,m} \xrightarrow{k_{fp}} \mathrm{D}_{b,n} + \mathrm{P}_{r+1,m} \tag{7}$$

Intramolecular Transfer (Short-Chain Branching).

$$P_{b,n} \xrightarrow{k_b} P_{b,n} \tag{8}$$

Random Scission.

$$\mathrm{P}_{b,n} + \mathrm{D}_{r,m} \xrightarrow{k_{sc}} \mathrm{D}_{b,n} + \mathrm{P}_{x,z} + \mathrm{D}_{r-x,m-z} \tag{9}$$

Termination by Combination.

$$\mathrm{P}_{b,n} + \mathrm{P}_{r,m} \xrightarrow{k_{tc}} \mathrm{D}_{b+r,n+m} \tag{10}$$

Termination by Disproportionation.

$$\mathrm{P}_{b,n} + \mathrm{P}_{r,m} \xrightarrow{k_{td}} \mathrm{D}_{b,n} + \mathrm{D}_{r,m} \tag{11}$$

The symbols $P_{b,n}$ and $D_{b,n}$ denote the respective "live" and "dead" polymer chains with "b" long-chain branches and a total chain length equal to "n". The above kinetic mechanism is quite general and includes the majority of elementary chemical reactions taking place in a free-radical polymerization system. According to the postulated kinetic mechanism, "live" polymer chains can terminate via termination by combination and disproportionation reactions as well as via transfer to monomer and solvent (chain transfer agent) reactions. Long-chain branches can be formed via transfer to "dead" polymer and terminal double-bond reactions while the intramolecular transfer reaction is responsible for the formation of short-chain branches in the polymer chains.

It should be noted that the postulated kinetic mechanism (i.e., eqs 1−11) has been widely employed in the literature[38−40]

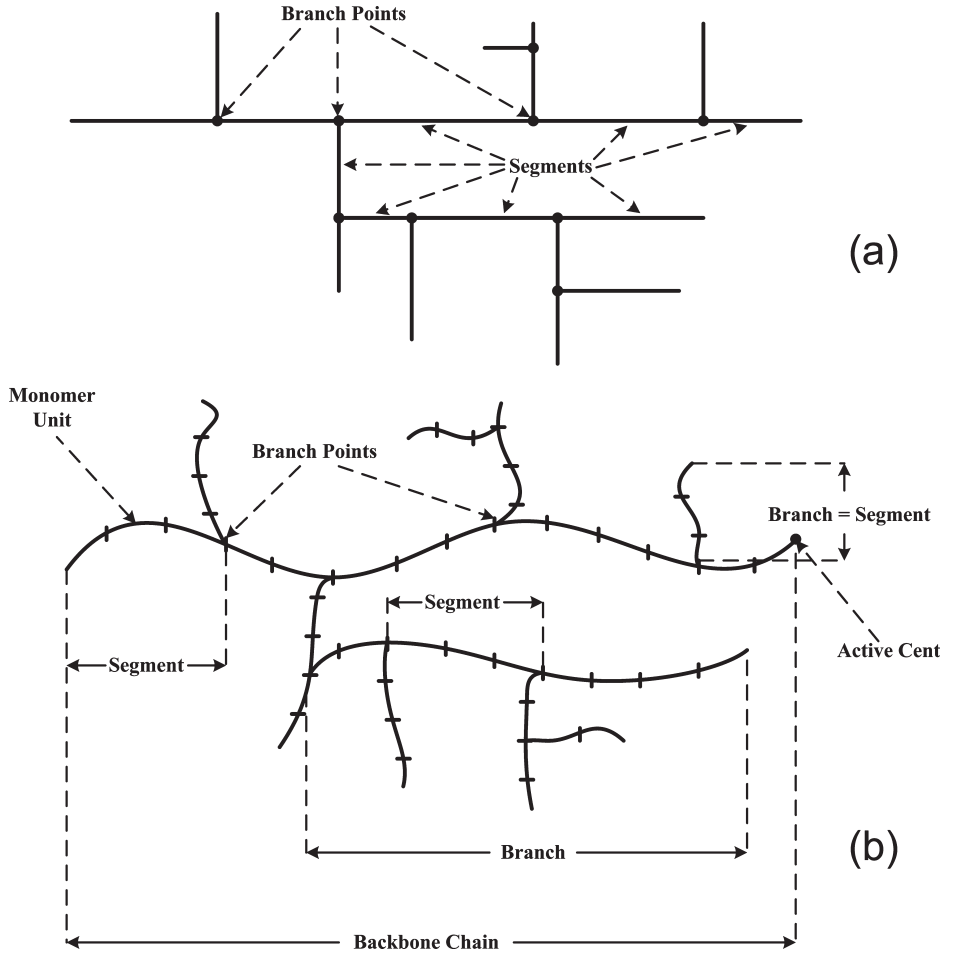

Figure 1. Schematic representation of a branched "live" polymer chain: (a) commonly adopted representation; (b) as defined in this work.

to describe the free-radical high-pressure polymerization of ethylene. The present mechanism does not include the production of polyradicals or the occurrence of intramolecular terminal double bond reactions. Moreover, the intramolecular transfer reaction (eq 8) was considered to exclusively produce butyl carbon groups[41,42] (i.e., via a hydrogen abstraction reaction to the fifth methylene group from the free-radical chain end). Any other reactions that may lead to the formation of different carbon groups (i.e., ethyl, vinyl, amyl, etc.) were not considered in the present study. However, as clearly described in the following section, additional reactions can easily be implemented provided that the numerical values of the respective kinetic rate constants are known.

The Stochastic Topology Algorithm

The dynamic evolution of a chemically initiated free-radical polymerization system can be accurately followed via a stochastic kinetic Monte Carlo (MC) approach. In a series of recent publications,[15,16] the development and application of a computationally efficient stochastic kinetic algorithm to free-radical dynamic polymerization systems has been described by the present authors. The proposed MC kinetic algorithm can accurately predict the average molecular properties (i.e., average molecular weights) as well as the distributed molecular properties (i.e., molecular weight, long-chain branching, copolymer composition and chain sequence length distributions, etc.) of the polymer chains in a dynamic polymerization system.

In the present work, a novel MC topology algorithm is described, on the basis of our previously published work,[15] to predict the exact topological molecular architecture of highly branched polymer chains. The basic principles governing the proposed MC formulation are described next. Prior to the detailed description of the topology algorithm, a brief overview of the terminology used in this work is presented.

In the majority of published papers, the analytical topology of polymer chains is visually described as a number of interconnected linear polymer parts, called ***segments*** (Figure 1a). These segments, also called 'primary polymers',[32] are randomly connected to form a polymer chain. Accordingly, the specific lengths of the various segments are calculated, as a function of the monomer conversion, by assuming that the various segments follow a-priori known segment "length distribution" (i.e., the most probable distribution). In the present work, a different approach is adopted to calculate the topological features of branched polymer chains in a time-varying polymerization system. More specifically, every branched polymer chain is considered to consist of a main ***backbone*** sequence of carbon atoms and a number of ***branches***, attached either to the main backbone chain or to any other branch of the highly branched polymer chain via a number of specific ***branching points*** (Figure 1b). The main backbone carbon sequence of atoms for a "live" polymer chain is assumed to be the only linear part of the highly branched structure with two free ends, one free end always representing the position of the propagating center of the "live" polymer chain. Upon deactivation of the "live" polymer chain, the resulting "dead" polymer chain is assumed to preserve its main structural characteristics. The size (length) of a fragment (i.e., segment) in a highly branched polymer chain is characterized by a number of ***monomer units*** (i.e., equal to its polymerization degree). The main difference between a branch and a segment

is that the former may contain a number of branch points while a segment is strictly bounded by two consecutive branch points or a branch point and a free end (see Figure 1b). In general, a branch can either contain several segments or be identical to the size of a single segment. It should be noted that the above definitions, specifically employed in the present study, greatly facilitate the identification of the various branched polymer chains in the stochastic topological algorithm and should not be confused with any other commonly employed definition (i.e., a "backbone chain" in a branched macromolecule commonly represents its longest linear part). Moreover, as will become clear in the following sections, the employed representation of a highly branched polymer chain is by no means unique and continuously undergoes topological transformations during the course of polymerization (e.g., Figure 7). The proposed polymer chain topological definitions are essential for the algorithm's functionality as well as for processing and explaining the stochastically calculated results.

A schematic representation of a "live" branched polymer chain, as defined in this work, is shown in Figure 1b. It is apparent that, following the present detailed chain representation, the various transformations a branched polymer chain undergoes during polymerization (see kinetic eqs 1−11) can be stochastically simulated, at the very low level of reacting monomer units.

To keep a complete record of all the topological features of a highly branched polymer chain, in a time-varying polymerization system, an elaborated numbering system to account for the exact position of all the monomer units in a polymer chain is required. To solve this extremely complex accounting problem, an efficient numbering algorithm has been developed based on the following general rules:

1. Each polymer chain is characterized by a unique sequence of consecutive numbers (i.e., from one to the total polymerization degree of a chain) that uniquely identify the positions of all the monomer units in a polymer chain.
2. The consecutive numbering of the monomer units in a branched polymer chain always initiates from its inactive free end of the backbone chain to the direction of its active free end.
3. The numbering of the monomer units in a branch follows the branch series appearance, always starting from the respective branching point to the free end of the branch.
4. Each time a polymer chain changes its state (i.e., reacts according to the kinetic mechanism, eqs 1−11), a new sequence of numbers are assigned to the new polymer chain.

The use of the above numbering rules to a typical branched polymer chain is shown in Figure 2. As can be seen, the assigned numbers are placed at the final connecting carbon atom of a monomer unit.

Following the above procedure, all the connecting points (i.e., bonds) in a polymer chain can be explicitly labeled. This allows the tracking of any new topological changes that may occur during the progress of polymerization. The topological information regarding a polymer chain is stored in the form of a column in the ***topology array***. This means that every branched polymer chain in the reacting mixture is represented by a column in the topology array. The top three rows in a topology column contain general information for the particular polymer chain, i.e., its total chain length, the length of its main "backbone" chain and the total number of branches. This information is necessary for later topological calculations. The subsequent rows in the topology column contain information regarding the exact length and

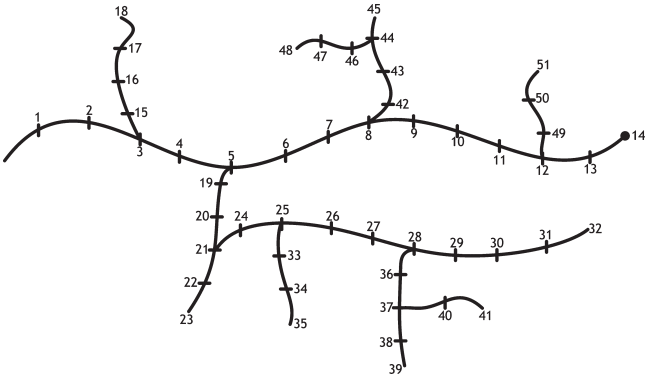

Figure 2. Numbering of a typical branched polymer chain, according to the established rules of the MC topology algorithm.

Table 1. Topology column corresponding to the polymer chain of Figure 2

row	stored topological information	value
1	total chain length	51
2	size of backbone chain	14
3	total number of branches (= b)	9
4	size of branch 1	4
5	position of branch 1	3
6	size of branch 2	5
7	position of branch 2	5
8	size of branch 3	9
9	position of branch 3	21
10	size of branch 4	3
11	position of branch 4	25
12	size of branch 5	4
13	position of branch 5	28
14	size of branch 6	2
15	position of branch 6	37
...	...	...
20 (= $(2b + 3) - 1$)	size of branch 9	3
21 (= $(2b + 3)$)	position of branch 9	12

position of all branches (i.e., short and long) in a branched polymer chain. The branch length and position of all the branches are stored in consecutive pairs in the topology column, following the branch series appearance. As a result, every time a new branch is formed in a polymer chain (e.g., due to a chain transfer to polymer reaction), the relevant information (i.e., branch length and position) is stored into predetermined places in the topology column. In Table 1, the elements of the topology column, corresponding to the polymer chain shown in Figure 2, are reported.

The proposed MC topology algorithm is based on the principle that the dynamic evolution of a polymer chain's microstructure can be inferred by simply tracking all the stochastically simulated reactions in the kinetic mechanism (i.e., eqs 1−11) and the corresponding changes they impart on the topological characteristics of the "live" and "dead" polymer chains. For example, when simulating the propagation reaction shown in Figure 3, the length of the main "backbone" chain increases by one monomer unit and so does the total length of the polymer chain. These changes are effected by changing the values of the relevant elements in the corresponding topology column of the polymer chain (i.e., rows 2 and 1, respectively) as well as the column elements corresponding to the positions of the branches that are not attached to the backbone chain (i.e., row 7), as shown in Figure 3.

A number of simple chemical reactions (e.g., transfer to monomer, transfer to solvent, termination by disproportionation, etc.) can be topologically simulated in a similar way. However, more complex chemical reactions, including termination by combination, transfer to polymer, etc., pose significant difficulties in their topological simulation. These difficulties are

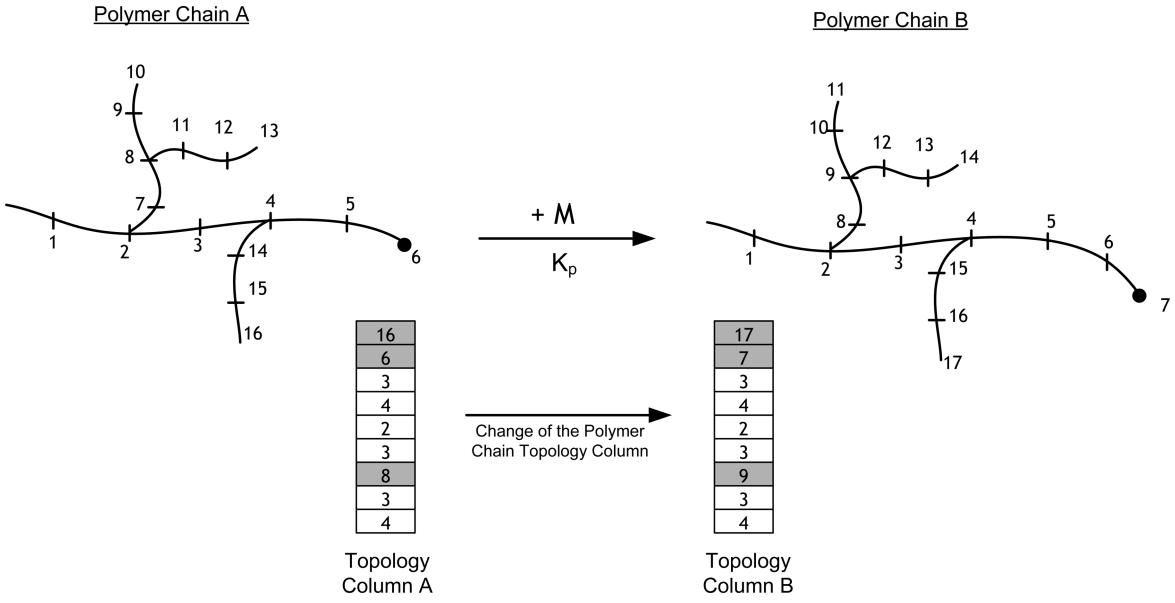

Figure 3. Stochastic topological simulation of a propagation reaction.

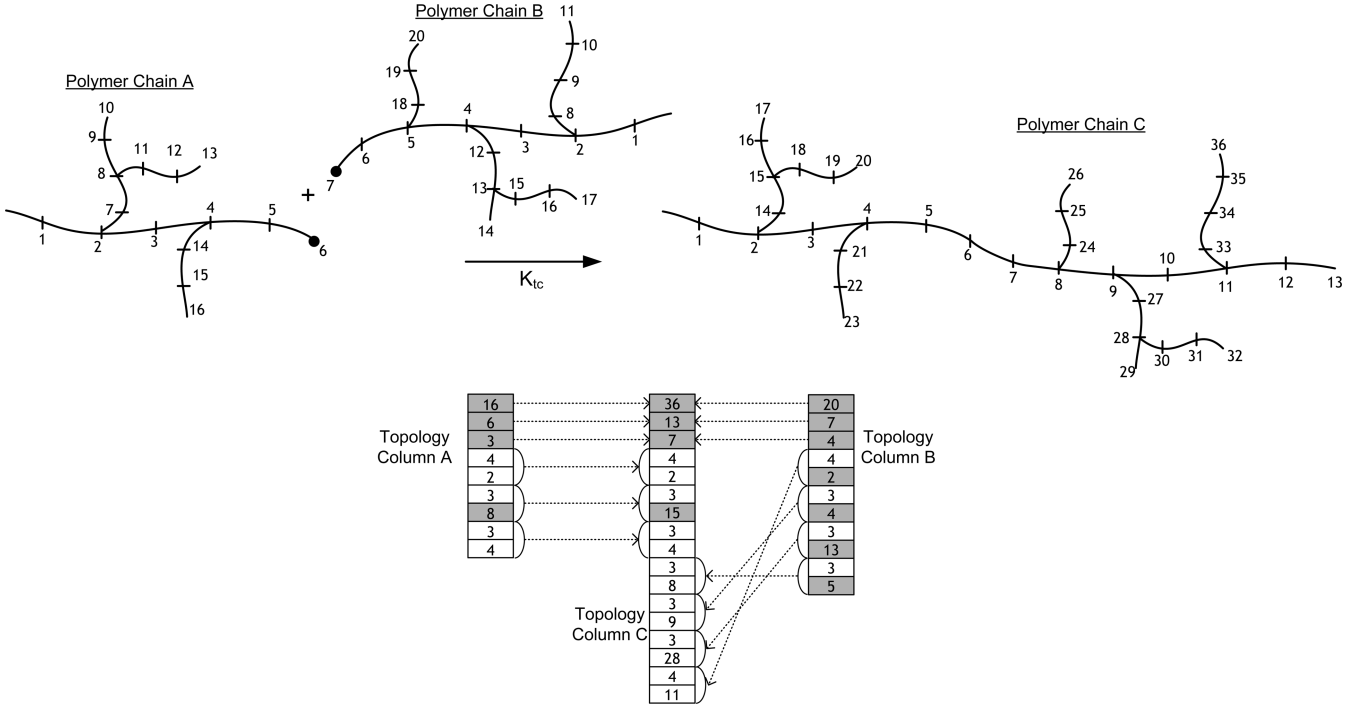

Figure 4. Stochastic topological simulation of a termination by combination reaction.

usually associated with the renumbering of a polymer chain or/and the reassignment of branching points. A typical example of renumbering of a polymer chain is shown in Figure 4, where the topological simulation of termination by combination reaction is depicted. As can be seen, the monomer units in the newly formed polymer chain (i.e., via the combination of two "live" polymer chains) are renumbered according to the general numbering rules defined above.

In Figure 5, the stochastic topological simulation of an intramolecular chain transfer reaction is depicted. In particular, the propagating center in a "live" polymer chain is moved from the chain's free end to a new position (i.e., to the fifth carbon atom from the chain's free end). As a result, renumbering of all the branching points that are not located on the main backbone chain is required. Similar difficulties are experienced with the topological simulation of a terminal double bond reaction, especially for highly branched polymer chains, as shown in Figure 6.

The topological simulation of a chain transfer to polymer reaction is by far the most complex one to follow since the produced polymer chains have completely different topologies from those of the two reacting chains. In Figure 7, the topological simulation of a chain transfer to polymer reaction is depicted. According to this reaction, the active center of a "live" polymer chain is transferred to an internal carbon atom of a "dead" polymer chain. Clearly, the new "live" polymer chain (i.e., formed via the chain transfer to polymer reaction) is characterized by a completely new topology column and, thus, a new (ab initio) numbering of the monomer units and branches of the generated "live" polymer chain is required.

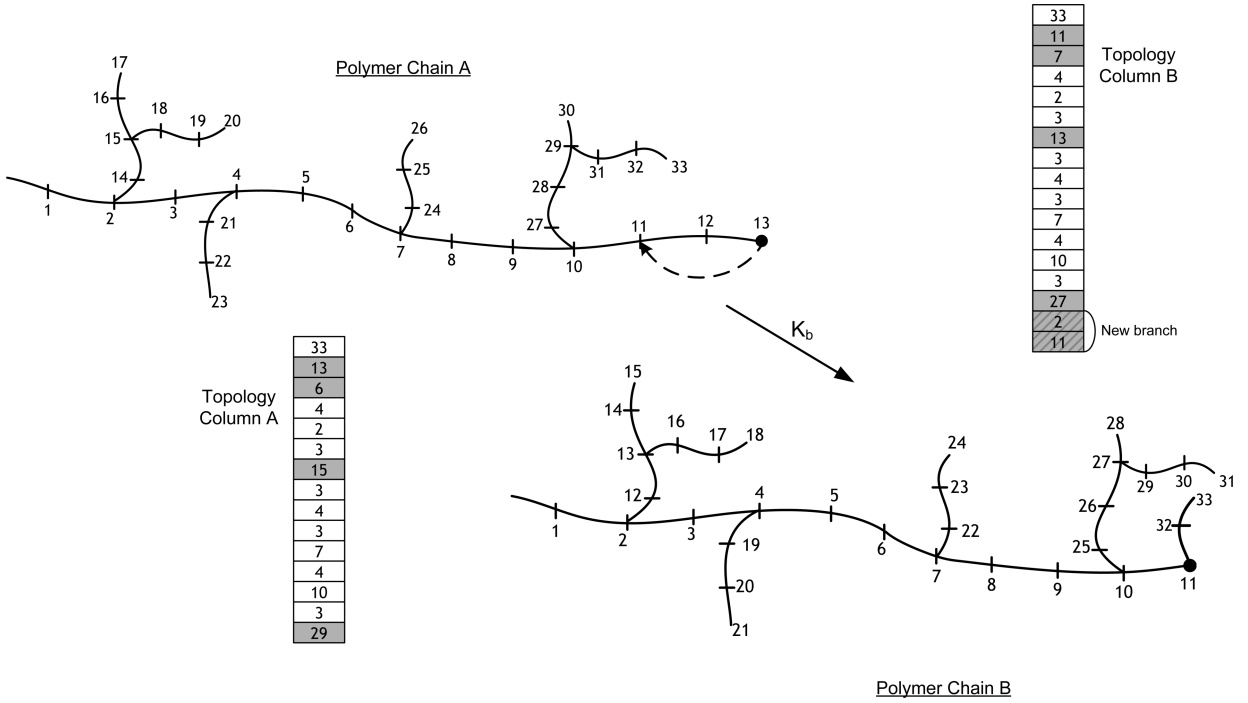

Figure 5. Stochastic topological simulation of an intramolecular transfer reaction.

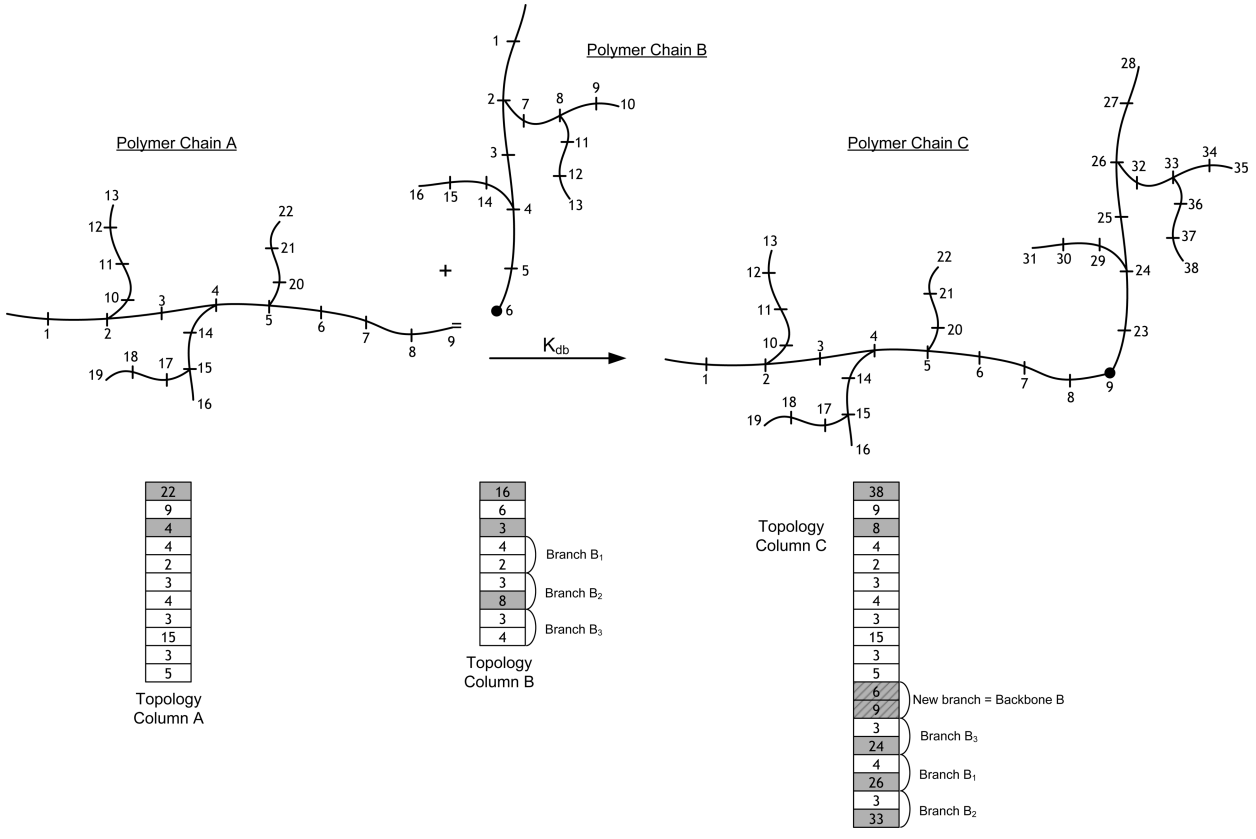

Figure 6. Stochastic topological simulation of a terminal double bond reaction.

From the above description of the MC topology algorithm, it becomes apparent that the algorithm's efficiency greatly depends on the efficient manipulation of the topology array since a huge amount of topological information needs to be dynamically accessed and/or changed in relation to the sample polymer chains population in a time-varying polymerization system. As a result, a large computational effort is required for the accurate bookkeeping of all the relevant topological features, a task far more difficult than the stochastic kinetic simulation of a polymeization system. To deal with this unique computational problem, a sophisticated array network has been developed to facilitate the quick and accurate tracking of all the stored topological information in

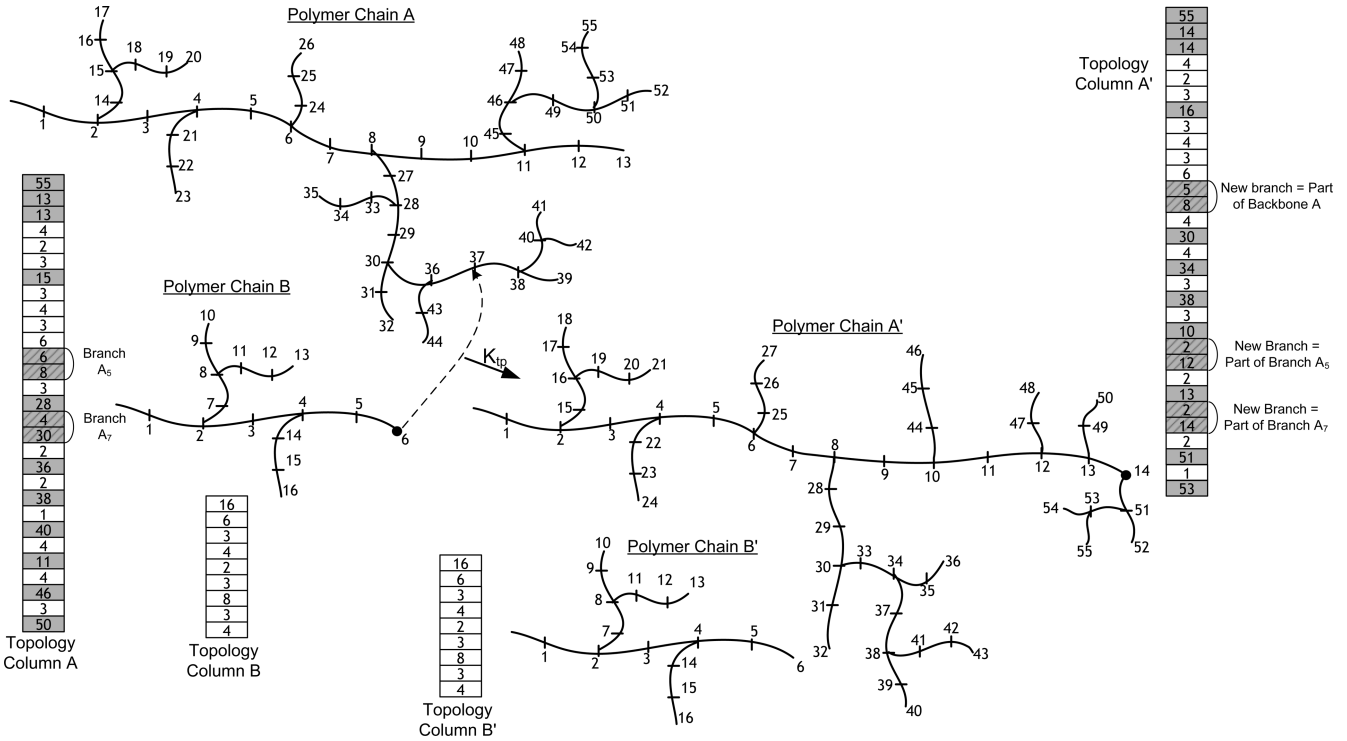

Figure 7. Stochastic topological simulation of a chain transfer to polymer reaction.

connection with all the simulated "live" and "dead" polymer chains in the sample population.

The Stochastic Kinetic Algorithm

The stochastic topology algorithm, responsible for the accurate accounting of all the topological features in relation to the polymer chains in a dynamic polymerization system, was combined with our well-established stochastic kinetic algorithm,[15,16] simulating all the chemical reactions in the kinetic mechanism (i.e., eqs 1−11). Note that the stochastic kinetic algorithm provides information on the net production/consumption rates of the various molecular species as well as on the molecular weight, degree of branching, etc., developments in the dynamic sample population. The calculated by the stochastic kinetic algorithm molecular properties (i.e., molecular weight, numbers of long- and short-chain branches, etc.) for each polymer chain in the sample population are stored in the two ***chain arrays***, corresponding to the "live" and "dead" polymer chains. Each column in the two chain arrays contains a number of molecular information (i.e., total degree of polymerization, number of long-chain branches per polymer chain, etc.), necessary for the molecular description of a polymer chain in the polymerization system. In order to link the MC kinetic algorithm with the stochastic topology algorithm, proper connections between the two chain arrays of the stochastic kinetic algorithm and the topology array in the stochastic topology algorithm have to be established. Accordingly, two ***position arrays*** are defined, containing information on the exact positions of the various "live" and "dead" polymer chains in the topology array. A schematic representation of the two position arrays is depicted in Figure 8. Thus, every time a new polymer chain is formed or an existing polymer chain changes its state (e.g., from "live" to "dead", etc.) the relevant entries in the position arrays (i.e., Pos(P) and Pos(D)) are updated so that an accurate connection between the polymer chain populations in the two kinetic chain arrays ("live" and "dead") and their corresponding topological information in the topology array is established.

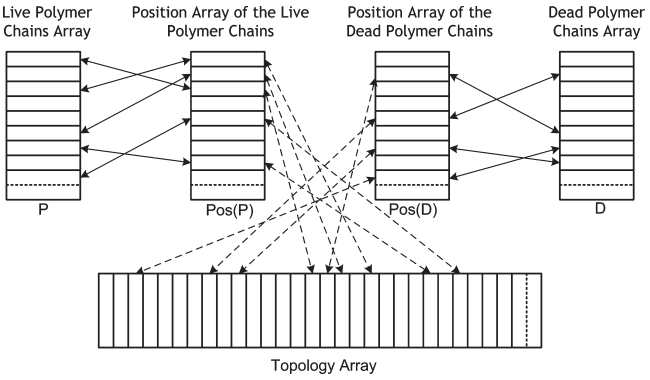

Figure 8. Schematic representation of the two "position arrays" used by the stochastic kinetic/topology algorithms.

From the above description it becomes evident that, based on the proposed stochastic kinetic/topology approach, the complete topological architecture of the polymer chains can be calculated in connection with the kinetic mechanism of a polymerization system. The fact that the kinetic part of the new topology algorithm remains identical to the already developed MC kinetic stochastic simulator[15,16] is an additional advantage of the new combined kinetic/topology approach. Thus, any changes in the kinetic mechanism are directly reflected into the calculated polymer chains topology. It should be noted that, contrary to previous efforts on the stochastic simulation of topological features of branched polymer chains, the present approach does not apply any simplifying assumption regarding the distributional forms of "live" and "dead" polymer chains populations. Moreover, the proposed stochastic method can take into account the effects of various diffusional limitations in the termination and propagation rate constants (i.e., gel- and glass-effect) as well as the effect of time-varying polymerization conditions (e.g., temperature, species concentrations, etc.).

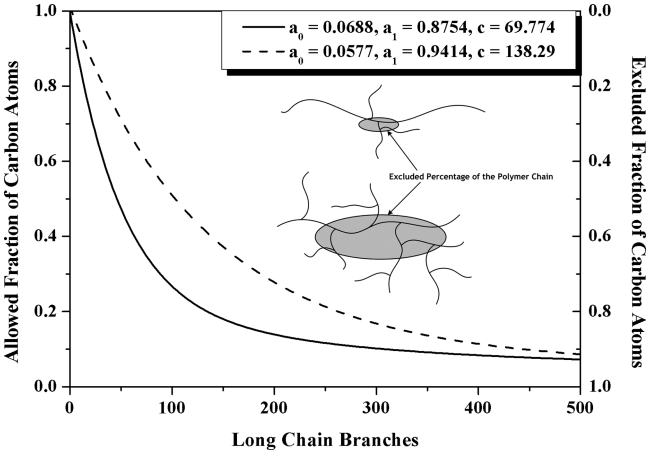

Figure 9. Effect of the LCB density on the excluded volume function. Inset: Schematic representation of the excluded volume of a branched polymer chain.

Another great novelty of the combined stochastic kinetic/topology algorithm is its ability to take into account various steric effects in highly branched polymer systems that can affect the kinetics of chain transfer to polymer and random scission reactions. In all previously published papers, chain scission and long-chain branching reactions have been treated as purely random events, meaning that all the carbon atoms in a highly branched polymer chain have the same probability for a radical attack to take place. This commonly employed assumption is made due to the inherent inability of the present deterministic and stochastic methods to numerically handle the solution of nonrandom kernels. In the present work, an excluded volume function was introduced to account for the effect of the branching density (see inserted scheme in Figure 9) on the chain scission and long-chain branching reactions. This means that in the excluded volume region the probability for a radical attack to a carbon atom decreases as the branching density increases. Thus, the excluded volume function allows the application of a nonequal probability function with regard to the stochastic simulation of chain scission and long-chain branching reactions. In general, the excluded volume in a highly branched polymer chain can be expressed as a function of the number of long-chain branches, b, per polymer chain:

$$f(b) = a_0 + a_1 \exp\left(-\frac{b}{c}\right) \tag{12}$$

where, a_0, a_1, and c are some constant parameters. The above expression can also be used to calculate the accessible polymer chain volume fraction for a random radical attack to take place. In Figure 9, eq 12 is plotted for two different sets of the parameters (a_0, a_1, and c). In the present study, all the stochastic simulations were carried out for the first set of parameter values shown in Figure 9.

It is apparent that an accurate description of the steric effects in a highly branched polymer reactive system requires a more detailed calculation of the excluded volume with respect to the local branching density of a polymer chain. However, such an approach increases dramatically the complexity and computational requirements of the stochastic algorithm (i.e., resulting in prohibitively high simulation times) and remains a challenging problem for future studies. Finally, it should be noted that steric effects due to the presence of short-chain branches were assumed negligible and, thus, were not included in the present study.

Table 2. Operating Conditions and Final Molecular Properties of LDPE

Mass Flow Rates of Feed and Side Streams (kg h^{-1})				
	feed stream	injection 1	injection 2	injection 3
ethylene	3×10^4	0.0	0.0	0.0
solvent[a]	209.8	0.0	0.0	0.0
initiator 1[a]	0.0	2.194	0.0	0.0
initiator 2[a]	0.0	1.615	0.768	1.230
initiator 3[a]	0.0	0.088	1.135	1.826

Average Molecular Properties			
	end of "zone 1"	end of "zone 2"	end of "zone 3"
M_n (g mol^{-1})	24.1×10^3	20.5×10^3	18.1×10^3
M_w (g mol^{-1})	11.7×10^4	15.4×10^4	18.3×10^4
LCB/1000C	0.85	1.8	3.0
SCB/1000C	8.2	9.3	10.1

[a] Undisclosed information due to confidentiality reasons.

Application of the MC Kinetic/Topology Algorithm to a High-Pressure LDPE Process

The proposed stochastic kinetic/topology algorithm is quite general and can be applied to different nonlinear polymerization systems, under the sole condition that their kinetic mechanism and kinetic rate constants are known. To demonstrate the predictive capabilities of the present stochastic approach, the free-radical polymerization of ethylene in a high-pressure tubular reactor was considered. The kinetic/topology algorithm was applied to a simulated model of a real industrial reactor of a total length of 1040 m. The tubular reactor included three initiator injection points and, thus, had three reaction zones. The reaction pressure at the reactor inlet was equal to 2700 atm. A detailed description of the high-pressure LDPE process can be found in a recent publication[43] while the operating conditions and the final average molecular properties of LDPE are reported in Table 2. The gel-effect model of Buback[44] was employed to describe the dependence of the termination rate constant on ethylene conversion. The kinetic rate constants, used in the present work, are reported in Table 3. The initial sample population for the MC kinetic/topology simulation contained 1.16×10^9 monomer molecules and 4.0×10^6 solvent molecules. It required approximately 96 min of simulation time, in a 2.21 GHz dual core processor (AMD Athlon 64 X2, 4200+). Furthermore, a detailed sensitivity analysis was carried out to assess the effect of the initial randomly selected condition on the predicted molecular properties. It was found that statistically accurate molecular properties and distributions were calculated by averaging the results of five randomly initialized consecutive MC simulation runs per case study, irrespectively of their specific starting point values. Note that, the effect of the initial sample size on MC simulation results has been discussed in detail in our previous publication.[15]

In the present tubular reactor study, the sample population is considered to be representative of the reaction mixture because of the ideal plug-flow assumption.[43] On the other hand, in an autoclave reactor case, in addition to the stochastic simulation of the polymerization kinetics one needs to take into account the residence time distribution of the sample population which significantly complicates the stochastic simulations. This is an interesting problem and a subject of a forthcoming study.

It must be noted here that the proposed MC algorithm, just like any discrete stochastic approach, possesses an inherent weakness regarding the sampling frequency of sparsely populated areas of the polymer chain distribution. This means that very large polymer chains (i.e., with a molecular weight larger than 10^6) are extremely difficult to be accurately represented in the MC sample population, due to their very low concentrations. In this case, no more than two polymer chains of such high molecular weight will

Table 3. Numerical Values of the Kinetic Rate Constants Used in the High-Pressure Free-Radical Polymerization of Ethylene

Kinetic Rate Constants: $k = k_0 \exp(-(E + P\Delta V)/(R\,T))$[a]			
reaction type	k_0 (L mol^{-1} s^{-1})	E (cal mol^{-1})	ΔV (cm^3 mol^{-1})
propagation	$k_{p0} = 2.59 \times 10^8$	$E_p = 9000.0$	$\Delta V_p = -19.7$
transfer to solvent	$k_{ts0} = 5.00 \times 10^{11}$	$E_{ts} = 17372.0$	$\Delta V_{ts} = -19.7$
transfer to polymer	$k_{tp0} = 1.0087 \times 10^9$	$E_{tp} = 12630.0$	$\Delta V_{tp} = 4.4$
intramolecular transfer	$k_{it0} = 4.80 \times 10^{8b}$	$E_{it} = 10570.0$	$\Delta V_{it} = -15.9$
β scission of *sec*-radicals	$k_{bssr0} = 4.015 \times 10^{7b}$	$E_{bssr} = 12080.0$	$\Delta V_{bssr} = -16.8$
β-scission of *tert*-radicals	$k_{bstr0} = 4.0125 \times 10^{7b}$	$E_{bstr} = 12080.0$	$\Delta V_{bstr} = -19.7$
random scission	$k_{sc0} = 3.70 \times 10^5$	$E_{sc} = 11080.0$	$\Delta V_{sc} = -16.8$
termination by combination	$k_{tc0} = 4.75 \times 10^9$	$E_{tc} = 1000.0$	$\Delta V_{tc} = 1.3$
termination by disproportionation	$k_{td0} = 1.55 \times 10^9$	$E_{td} = 1000.0$	$\Delta V_{td} = 1.3$

[a] The symbols P and R denote the reactor pressure and the universal gas constant, respectively. [b] Measured in sec^{-1}

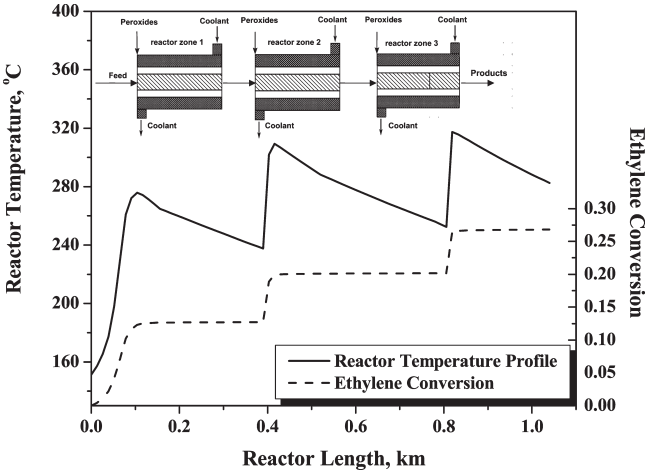

Figure 10. Calculated reaction temperature and ethylene conversion profiles along the reactor length.

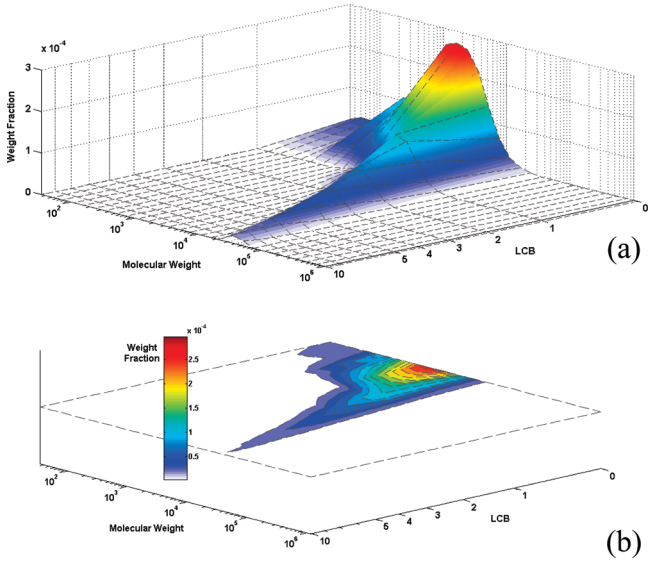

Figure 11. Calculated (a) 2-D joint (LCB−MW) distribution and (b) respective contour plots of LDPE at the reactor exit, using a sample population of 4.9×10^4 branched polymer chains.

be usually present in the final sample population. Nevertheless, a total mass consistency check (i.e., the total mass in the stochastic system is preserved, and its value is compared with the total mass calculated by other independent methods) in combination with the use of multiple stochastic simulations per case study, minimize the effect of this problem on the overall accuracy of the proposed kinetic/topology method. Moreover, as the quest for conceptually more efficient approaches continues, the constant increase in computer capabilities gradually diminishes any serious drawbacks in the application of stochastic approaches.

In Figure 10, the reaction temperature profile and the ethylene conversion along the reactor length are depicted. As can be seen, there are three distinct temperature peaks corresponding to the three reaction zones (i.e., three initiator injection points).

In Figure 11a, the 2-D long-chain branching−molecular weight (LCB−MW) distribution of low-density polyethylene (LDPE) calculated at the reactor exit, is depicted. The 2-D distribution provides detailed information on the number of long-chain branches of LDPE with respect to its molecular weight. In particular, it predicts the distribution of the mass fractions of the polymer chains with respect to their molecular weight for a given value of LCBs per molecule as well as the distribution of the mass fractions of polymer chains with respect to the number of LCBs per molecule for a given value of molecular weight. The definition and calculation of the above distributions are described in detail in a recent publication by the same authors.[15] The respective contour plots of the bivariate (LCB−MW) distribution are presented in Figure 11b. It is clear that the largest fraction of the polymer chains will have 1−3 LCBs per molecule. Moreover, as the number of LCBs per molecule increases the respective weight fraction of the branched polymer chains decreases while, at the same time, the corresponding distribution becomes narrower (see Figure 11, parts a and b). It should be pointed out that it is the first time that the calculation of the 2-D joint (LCB−MW) distribution is reported in the literature for a high-pressure tubular LDPE industrial reactor.

Similar information on the joint short-chain branching−molecular weight (SCB−MW) distribution of LDPE is presented in Figure 12, parts a and b. As can be seen, the largest fraction of the polymer chains will have 1−10 SCBs per molecule. Both distributions (i.e., (LCB−MW) and (SCB−MW) distributions) show a long tail (i.e., polymer chains with a high content in both LCB and SCB) at high molecular weights. It is also evident that the peak value of (LCB−MW) distribution is higher than the corresponding peak value of (SCB−MW) distribution and exhibits a sharper decrease with respect to the branching content.

In Figure 13, parts a and b, the stochastically calculated joint long-chain branching−short-chain branching (LCB−SCB) distribution of LDPE and the respective contour plots are depicted. The (LCB−SCB) distribution represents the fraction of polymer chains with specific numbers of long-chain and short-chain branches per molecule and is in complete agreement with the respective results of Figures 11 and 12 on (LCB−MW) and (SCB−MW) distributions.

In Figure 14, the number of long- and short-chain branches distributions per 1000 carbon atoms are plotted. It should be noted that similar results have been reported by Iedema.[12] This information can be directly compared with respective C NMR experimental measurements and ultimately lead to a realistic

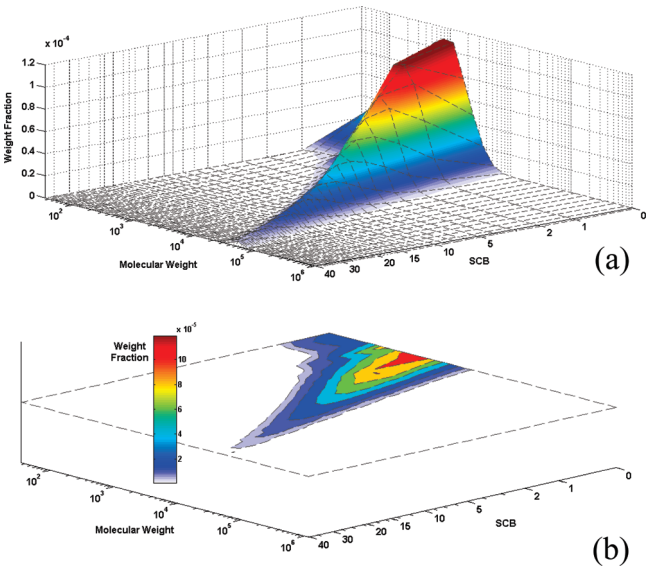

Figure 12. Calculated (a) 2-D joint (SCB−MW) distribution and (b) respective contour plots of LDPE at the reactor exit, using a sample population of 4.9×10^4 branched polymer chains.

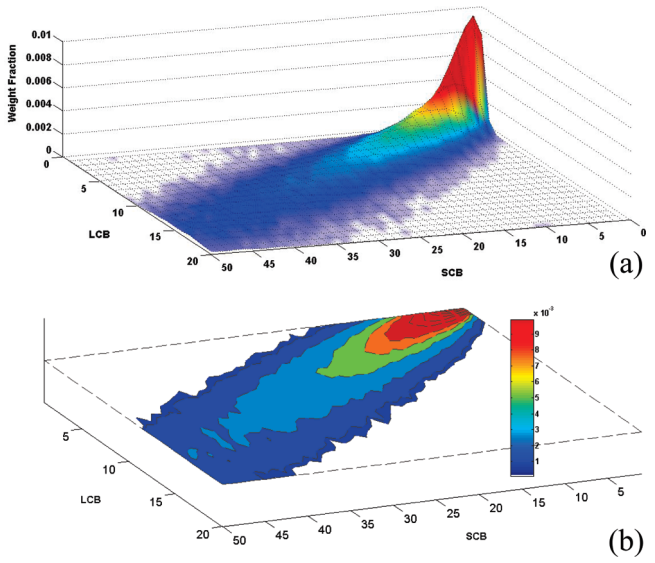

Figure 13. Calculated (a) 2-D joint (LCB−SCB) distribution and (b) respective contour plots of LDPE at the reactor exit, using a sample population of 4.9×10^4 branched polymer chains.

prediction of the physical (i.e., prediction of the polymer density or/and crystallinity with respect to the molecular weight) and rheological properties of LDPE.

Another molecular property of interest for highly branched polymer chains, directly calculated by the present stochastic kinetic/topology algorithm, is the average length distribution of long-chain branches with respect to the total chain length (or molecular weight) of the polymer chains. In Figure 15, the average length of LCBs (i.e., branch length distribution, BLD) of LDPE at the exit of the tubular reactor, is illustrated. As can be seen, the mean size of long-chain branches increases with respect to the total length (molecular weight) of the polymer chains. Note that a similar behavior was reported for the average LCB length by several investigators[45,46] who experimentally measured with the aid of C NMR the average LCB length for various LDPE grades.

The branching structure in highly branched polymer chains is commonly characterized by the number of consecutive "branching order levels". In the present study, every branch that is directly attached to the main carbon backbone chain is defined as zero-order branch. A branch attached to a zero-order branch is characterized as a first-order branch while a branch of order "$n+1$" is a branch attached to an "n" order branch. Thus, another property of interest that can be obtained from our stochastic kinetic/topology algorithm, is the bivariate branching order−branch molecular weight (BO−BMW) distribution. In Figure 16, parts a and b, the bivariate (BO−BMW) distribution of LDPE and the respective contour plots, as calculated by our MC kinetic/topology algorithm at the reactor exit, are shown. One can easily observe the appearance of two distinct distributions, a narrow one in the low molecular weight region, corresponding to the short-chain branches, and a broader one in the high molecular weight region, corresponding to the long-chain branches. Both distributions reveal that the "branching order levels" of the majority of long- and short-chain branches are in the range of 0−3.

In a number of recent publications[28−31] it has been shown that the topology of branched polymer chains is directly linked with the rheological behavior of the polymer melt. In fact, Read and McLeish[47] were among the first ones who used the terms ***seniority*** and ***priority*** to characterize the branching topology of a branched polymer chain. The seniority[48] of a segment in a branched polymer chain can be calculated by counting the total number of segments starting from the segment of interest to the furthest

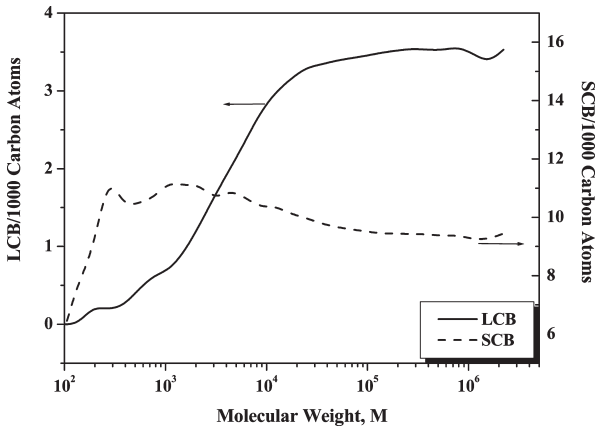

Figure 14. Number distributions of long- and short-chain branches per 1000 carbon atoms of LDPE, calculated by the stochastic kinetic/topology algorithm at the reactor exit.

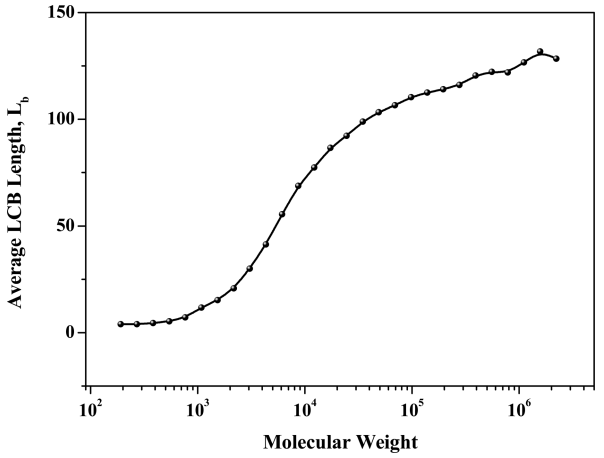

Figure 15. Average long-chain branch length distribution (BLD) of LDPE, calculated by the stochastic kinetic/topology algorithm at the reactor exit.

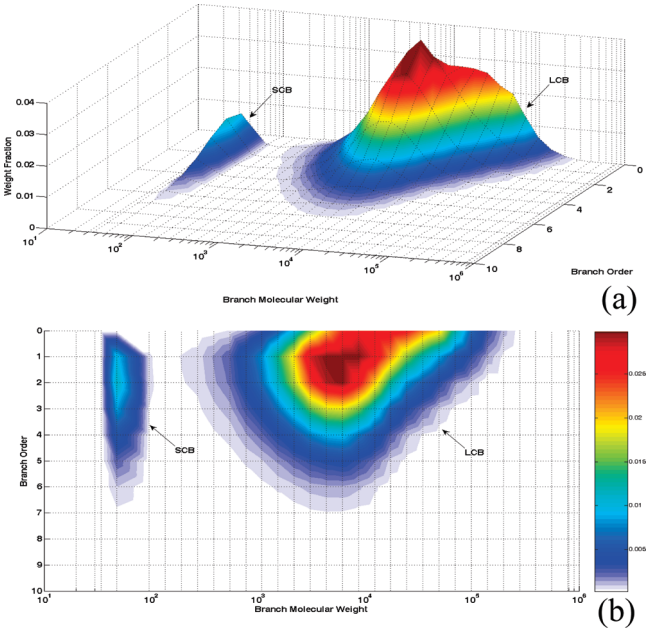

Figure 16. Calculated (a) bivariate (BO−BMW) distribution and (b) respective contour plots of LDPE at the reactor exit, using a sample population of 4.9×10^4 branched polymer chains.

polymer chain end on both sides of the segment and taking the smallest of the two calculated values. Note that the seniority of a segment is related to its respective relaxation time. On the other hand, the priority[49] of a segment in a branched polymer chain is related to its maximum stretch and is calculated by counting the free arms attached to each side of the segment and taking the smallest of the two values.

In Figure 17, the calculated seniority and priority segment number fraction distributions of LDPE, produced in a three-zone high-pressure tubular reactor, are depicted. The seniority and priority segment number fraction distributions provide valuable information on the branching structure of highly branched polymer chains (i.e., higher seniority and priority values reveal the existence of a more highly branched polymer structure while, similar seniority and priority values show that the structure of the branched polymer chains is closer to that of an ideal comb-type topology[47]).

Calculation of the Radius of Gyration

On the basis of the calculated topologies of LDPE chains, one can easily reconstruct their respective 3-D spatial configurations using a standard random-walk molecular simulator.[50] In the present study, molecular simulations were carried out under Θ-solvent conditions (i.e., no interactions with solvent molecules were considered, neither any nearest neighbor interactions were introduced) to reconstruct the 3-D spatial configurations of the LDPE chains. The molecular simulation was based on a random stepwise addition of consecutive monomer units, using specific directional rules (i.e., the step-direction of the simulations can be dictated either by cubic[51,52] or tetrahedral[53] formulation rules).

The reconstruction of the spatial configurations of the LDPE chains was based on the detailed topological information provided by our novel stochastic kinetic/topology algorithm. Topological information on the exact size of every part of the polymer chain (i.e., backbone chain, long- or short-chain branches) was used to determine the number of steps required by the molecular simulation algorithm for the reconstruction of a chain part, while the position of the branch points provided the initial coordinates

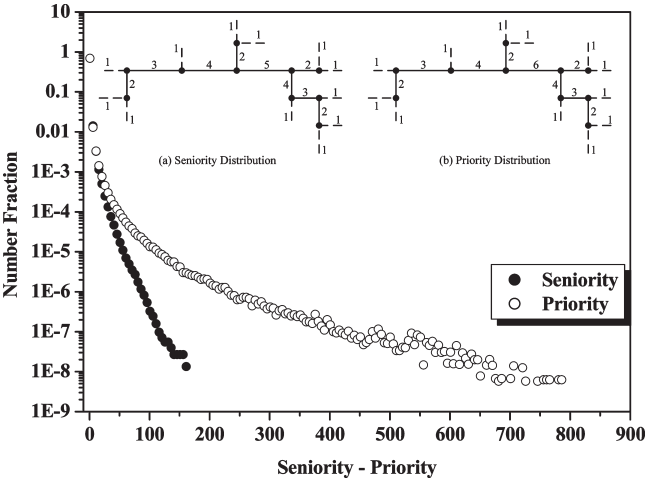

Figure 17. Seniority and priority segment number fraction distributions of LDPE, (calculated by the stochastic kinetic/topology algorithm at the reactor exit). The inset schemes denote the segment seniority and priority values in a branched polymer chain.

for the simulation of the various branches. Following the above procedure, random 3-D configurations of the LDPE chains were obtained.

It should be noted that the sole purpose of the present application was to demonstrate the potential of our novel stochastic kinetic/topology algorithm to provide the necessary topological information for the calculation of important spatial molecular properties of highly branched polymer chains. It must be emphasized that a number of approaches (e.g., self-avoiding walk, incomplete enumeration, excluded volume interactions, bond rotation potentials, coarse grained approaches, etc.) can be employed to calculate the 3-D spatial configuration of highly branched polymer chains. These methods are characterized by a number of advantages and disadvantages with regard to their efficiency, statistical accuracy, computational speed, etc. Thus, the selection of a molecular 3-D simulation method largely depends on the final application objectives.[54]

Thus, using the calculated chain topologies of LDPE molecules and a random-walk molecular simulation algorithm, the exact 3-D spatial configurations of the highly branched polymer chains can be obtained. Accordingly, a number of important properties, associated with the volume occupied by a polymer chain, can be calculated. More specifically, it is possible to calculate the mean radius of gyration, R_g, and the mean hydrodynamic radius, R_h, of branched polymer chains, using the following expressions:

$$R_g^{\,2} = (2N^2)^{-1}\left\langle \sum_{i=1}^{n}\sum_{j=1}^{n} r_{ij}^{\,2}\right\rangle;$$

$$(R_h)^{-1} = (2N^2)^{-1}\left\langle \sum_{i=1}^{n}\sum_{\substack{j=1\\ i\neq j}}^{n} r_{ij}^{\,-1}\right\rangle \qquad (13)$$

where the symbols r_{ij} and N denote the distance between the monomer units "i" and "j" in a 3-D statistically reconstructed polymer chain and the total number of steps (i.e., monomer units), respectively. The brackets ($< >$) denote the mean statistical ensemble based on a number of molecular simulations carried out for the same polymer chain.

In Figure 18, the predicted values of the mean radius of gyration, R_g, for a sample of 4.9×10^4 LDPE chains, are plotted with respect to the chain length. Each red point in Figure 18

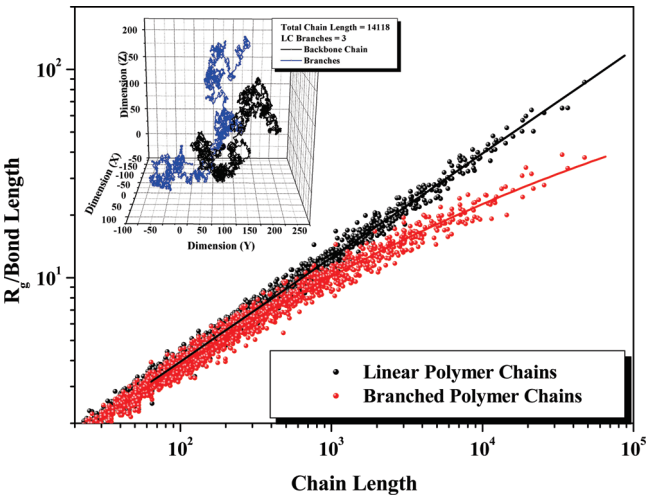

Figure 18. Calculated values of the mean radius of gyration for LDPE and linear polymer chains of the same molecular weight.

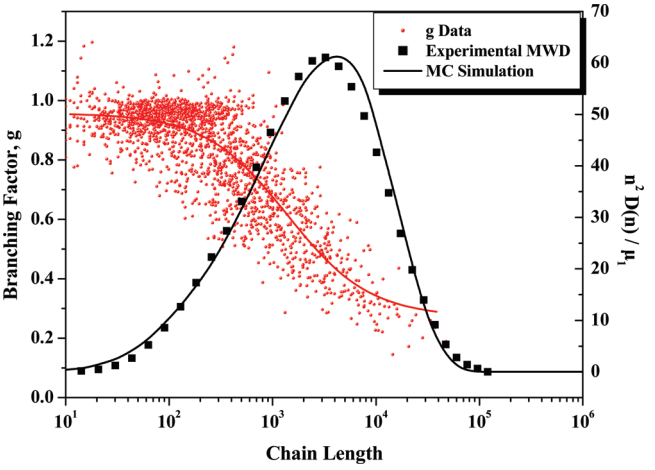

Figure 19. Experimental and predicted MWDs of LDPE (calculated at the reactor exit) and the effect of molecular weight of LDPE on the branching factor, *g*.

represents the average (arithmetic mean) of 10 successive molecular simulations carried out for every single branched polymer chain in the sample population. The black points in Figure 18 represent the respective values of R_g for linear polymer chains with molecular weights equal to the respective values of the branched polymer chains. As expected, the calculated average values of R_g for the linear polymer chains are higher than those for the branched polymer chains of the same molecular weight. It should be noted that the slope of the curve, representing the variation of R_g with respect to the chain length for linear polymer chains was found to be equal to 0.4994, which is very close to the theoretical one (i.e., 0.5).[54,55] On the other hand, the slope of the curve representing the variation of R_g values with respect to the chain length of branched polymer chains, was found to be equal to 0.2511, in the high chain length region, which is in perfect agreement with the theoretically reported value for randomly branched polymer chains in Θ-solvent (i.e., 0.25).[54,55]

The maximum chain length of the simulated linear and nonlinear polymer chains was equal to 6.457×10^4 monomer units while the maximum number of long- and short-chain branches in a polymer chain was equal to 1832. The 3-D simulation required approximately 21 h in a 1.6 GHz quad core processor (Intel Xeon 5110). All the 3-D molecular simulations were carried out assuming a cubic spatial configuration for the simulated polymer chains. In the inserted scheme of Figure 18, the 3-D configuration of a branched polymer chain with three long-chain branches and a total chain length equal to 14118 monomer units is depicted.

Another parameter that reflects the extent of long-chain branching in LDPE and is strongly related with the rheological behavior of an LDPE melt, is the branching factor, *g*:

$$g = \left(\frac{\overline{R_g^2}_{br}}{\overline{R_g^2}_{lin}} \right)_M \qquad (14)$$

The indexes "br" and "lin" denote the respective branched and linear polymer chains with the same molecular weight.

In Figure 19, the experimentally measured MWD is compared with the calculated one at the exit of an industrial high-pressure, three-zone tubular reactor. As can be seen, the MC calculated MWD is in excellent agreement with the experimentally measured distribution. In the same figure, the variation of the branching factor, g, with respect to the molecular weight of LDPE is depicted. To our knowledge, it is the first time that the variation of the branching factor, g, with respect to the polymer chain length is reported, based on such detailed kinetic/topological molecular calculations.

Conclusions

In the present work, a novel stochastic kinetic/topology stochastic algorithm is described for the accurate prediction of the complete topological architecture of highly branched polymer chains. Stochastic topological simulations were carried out in conjunction with a stochastic kinetic simulator. It should be noted that, contrary to previous efforts on the stochastic simulation of topological features of branched polymer chains, the present approach does not require any simplifying assumptions regarding the distributional forms of "live" and "dead" polymer chain populations. Moreover, the proposed stochastic approach can explicitly take into account the effects of various diffusional limitations in the termination and propagation rate constants (i.e., gel- and glass-effect) as well as of time-varying polymerization conditions on kinetic/topology developments in highly nonlinear polymerization systems. The effect of branching density on the kinetics of various reactions (i.e., transfer to polymer and chain scission reactions) was also examined via the introduction of a semiempirical excluded volume function.

To demonstrate the predictive capabilities of the proposed stochastic approach, the free-radical polymerization of ethylene (LDPE) in an industrial high-pressure tubular reactor was investigated. Through this study, the kinetic/topology algorithm revealed detailed information on the branching structure (i.e., (LCB−MW), (SCB−MW), (LCB−SCB) distributions, BL distribution, number of long- and short-chain branches per 1000 carbon atoms distributions, (BO−BMW) distribution, seniority and priority segment number fraction distributions) of LDPE.

Subsequently, the topological information obtained by the application of the stochastic kinetic/topology algorithm was used in conjunction with a 3-D molecular random-walk simulation algorithm to predict the 3-D random spatial configurations of the branched polymer chains and, thus, to calculate some important rheological parameters (i.e., the mean radius of gyration, R_g, the mean hydrodynamic radius, R_h, and the average branching factor, *g*) of highly branched polymer chains.

References and Notes

(1) Kiparissides, C. *J. Process Control* **2006**, *16*, 205–224.
(2) Crowley, T. J.; Choi, K. Y. *Ind. Eng. Chem. Res.* **1997**, *36*, 1419–1423.
(3) Crowley, T. J.; Choi, K. Y. *Ind. Eng. Chem. Res.* **1997**, *36*, 3667–3684.

(4) Yoon, W. J.; Ryu, J. H.; Cheong, C.; Choi, K. Y. *Macromol. Theory Simul.* **1998**, *7*, 327–332.
(5) Tobita, H.; Ito, K. *Polym. React. Eng.* **1993**, *1*, 407–418.
(6) Nele, M.; Sayer, C.; Pinto, J. C. *Macromol. Theory Simul.* **1999**, *8*, 199–213.
(7) Achilias, D. S.; Kiparissides, C. J. *Macromol. Sci., Rev. Macromol. Chem. Phys.* **1992**, *C32*, 183–234.
(8) Baltsas, A.; Achilias, D.; Kiparissides, C. *Macromol. Theory Simul.* **1996**, *5*, 477–497.
(9) Teymour, F.; Cambell, J. D. *Macromolecules* **1994**, *27*, 2460–2469.
(10) Pladis, P.; Kiparissides, C. *Chem. Eng. Sci.* **1998**, *53*, 3315–3333.
(11) Wulkow, M. *Macromol. Theory Simul.* **1996**, *5*, 393–416.
(12) Iedema, P. D.; Wulkow, M.; Hoefsloot, H. C. J. *Macromolecules* **2000**, *33*, 7173–7184.
(13) Kumar, S.; Ramkrishna, D. *Chem. Eng. Sci.* **1996**, *51*, 1311–1332.
(14) Saliakas, V.; Chatzidoukas, C.; Krallis, A.; Meimaroglou, D.; Kiparisides, C. *Macromol. React. Eng.* **2007**, *1*, 119–136.
(15) Meimaroglou, D.; Krallis, A.; Saliakas, V.; Kiparissides, C. *Macromolecules* **2007**, *40*, 2224–2234.
(16) Krallis, A.; Meimaroglou, D.; Kiparissides, C. *Chem. Eng. Sci.* **2008**, *63*, 4342–4360.
(17) Gillespie, D. T. *J. Phys. Chem.* **1977**, *81*, 2340–2361.
(18) Tobita, H. *J. Polym. Sci., Phys. Ed.* **1993**, *31*, 1363–1371.
(19) Lu, J.; Zhang, H.; Yang, Y. *Macromol. Chem., Theory Simul.* **1993**, *2*, 746–760.
(20) He, J.; Zhang, H.; Yang, Y. *Macromol. Tehory Simul.* **1995**, *4*, 811–819.
(21) He, J.; Zhang, H.; Chen, J.; Yang, Y. *Macromolecules* **1997**, *30*, 8010–8018.
(22) Xu, G. *J. Polym. Sci.: B. Polym. Phys.* **1997**, *35*, 1161–1166.
(23) Costeux, S.; Anantawaraskul, S.; Wood-Adams, P. M.; Soares, J. B. P. *Macromol. Theory Simul.* **2002**, *11*, 326–341.
(24) Anantawaraskul, S.; Soares, J. B. P.; Wood-Adams, P. M. *Macromol. Theory Simul.* **2003**, *12*, 229–236.
(25) Al-Saleh, M. A.; Simon, L. C. *Macromol. Symp.* **2006**, *243*, 123–131.
(26) McLeish, T. C. B.; Larson, R. G. *J. Rheol.* **1998**, *42*, 81–110.
(27) Majeste, J. C.; Carrot, C.; Stanescu, P. *Rheol. Acta* **2003**, *42*, 432–442.
(28) Das, C.; Inkson, N. J.; Read, D. J.; Kelmanson, M. A.; McLeish, T. C. B. *J. Rheol.* **2006**, *50*, 207–234.
(29) Park, S. J.; Larson, R. G. *J. Rheol.* **2005**, *49*, 523–536.
(30) Park, S. J.; Shanbhag, S.; Larson, R. G. *Rheol. Acta* **2005**, *44*, 319–330.
(31) Inkson, N. J.; McLeish, T. C. B.; Harlen, O. G.; Groves, D. J. *J. Rheol.* **1999**, *43*, 873–896.
(32) Tobita, H.; Hatanaka, K. *J. Polym. Sci., Polym. Phys. Ed.* **1996**, *34*, 671–681.
(33) Tobita, H. *J. Polym. Sci., B: Polym. Phys.* **2001**, *39*, 391–403.
(34) Inkson, N. J.; Das, C.; Read, D. *Macromolecules* **2006**, *39*, 4920–4931.
(35) Iedema, P. D.; Hoefsloot, H. C. J. *Macromol. Theory Simul.* **2001**, *10*, 855–869.
(36) Kim, D.; Busch, M.; Hoefsloot, H. C. J.; Iedema, P. D. *Chem. Eng. Sci.* **2004**, *59*, 699–718.
(37) Iedema, P. D.; Wulkow, M.; Hoefsloot, H. C. J. *Polymer* **2007**, *48*, 1770–1784.
(38) Zabisky, R. C.; Chan, W. M.; Gloor, P. E.; Hamielec, A. E. *Polymer* **1992**, *33*, 2243–2262.
(39) Kiparissides, C.; Verros, G.; McGregor, J. F. *J. Macromol. Sci.—Rev. Macromol. Chem. Phys.* **1993**, *C33*, 437–527.
(40) Pladis, P.; Kiparissides, C. *Chem. Eng. Sci.* **1998**, *53*, 3315–3333.
(41) Roedel, M. J. *J. Am. Chem. Soc.* **1953**, *75*, 6110–6112.
(42) Odian, G. In *Principles of Polymerization*; John Wiley and Sons: New York, 1981; p 241.
(43) Kiparissides, C.; Baltsas, A.; Papadopoulos, S.; Congalidis, J. P.; Richards, R.; Kelly, M. B.; Ye, Y. *Ind. Eng. Chem. Res.* **2005**, *44*, 2592–2605.
(44) Buback, M. *Macromol. Chem.* **1990**, *191*, 1575–1587.
(45) Bugada, D. C.; Rudin, A. *J. Appl. Polym. Sci.* **1987**, *33*, 87–93.
(46) Usami, T.; Gotoh, Y.; Takayama, S. *J. Appl. Polym. Sci.* **1991**, *43*, 1859–1863.
(47) Read, D. J.; McLeish, T. C. B. *Macromolecules* **2001**, *34*, 1928–1945.
(48) Rubinstein, M.; Zurek, S.; McLeish, T. C. B.; Ball, R. C. *J. Phys. (Fr.)* **1990**, *51*, 757–775.
(49) Bick, D. K.; McLeish, T. C. B. *Phys. Rev. Let.* **1996**, *76*, 2587–2590.
(50) Tobita, H.; Hamashima, N. *J. Polym. Sci., B: Polym. Phys.* **2000**, *38*, 2009–2018.
(51) Wall, F. T.; Hiller, L. A. *J. Chem. Phys.* **1954**, *22*, 1036–1041.
(52) Rosenbluth, M. N.; Rosenbluth, A. W. *J. Chem. Phys.* **1955**, *23*, 356–359.
(53) Mills, L. J. *Plastics: Microstructure and engineering applications*; Elsevier Science and Technology Books: New York, 2005; p 58.
(54) Binder, K. *Monte Carlo and Molecular Dynamics Simulations in Polymer Science*; Oxford University Press: Oxford, U.K., 1995.
(55) Rubinstein, M.; Colby, R. H. *Polymer Physics*; Oxford University Press: Oxford, U.K., 2003.